2019

Effects of SUV39H1 and SUV420H1/H2 on Programmed Genome Rearrangement in *Petromyzon marinus*

Claire A. Scott
University of Kentucky

Notes:
Claire Scott won the first place in the Biological Sciences category.

Introduction

The sea lamprey, a jawless vertebrate, diverged from the vertebrate lineage approximately 550 million years ago. This deep shared ancestry between sea lamprey and all other living vertebrates presents a powerful evolutionary model for understanding how epigenetic mechanisms (including histone methylation and programmed genome rearrangement) evolved during early vertebrate ancestry. A unique regulatory mechanism, known as programmed genome rearrangement (PGR), occurs in sea lamprey (*Petromyzon marinus)* and hagfish (another ancient lineage of jawless fish). In lamprey, PGR results in the reproducible elimination of approximately 20% of the genome from somatic cells, with this material only being retained by germline cells. PGR occurs in many taxa including protozoan, invertebrate and vertebrate taxa, resulting in a variety of mechanisms with a common theme, germline-specific genomes [1]. The deleted genome is necessary for germline development and maintenance, genes that if misexpressed will result in oncogenesis in somatic cells [2]. Related to this, one other important feature of sea lamprey biology is their ability to regain full spinal cord function after injury, which might potentially be contributed by pluripotency of somatically resident germline-like cells. Genes involved with pluripotency functions are highly valuable in the context of early embryogenesis, regeneration and gamete production, but when misexpressed in "normal" somatic cells these same genes may become deleterious, demonstrated through resulting oncogenesis when overexpressed [3].

Programmed genome rearrangement is initiated in early embryogenesis, specifically day 2 post fertilization [3]. In lamprey, PGR can be seen directly in anaphase of mitosis. When DNA is separated across the metaphase plate, pulled to opposite ends of the cell, some DNA is left behind as shown in Figure 1. This lagging chromatin is therefore not placed in the nucleus (as is the case for the rest of the somatic DNA), instead it is packaged into smaller vesicles known as "micronuclei." After the completion of mitosis and the creation of the micronuclei, they are found in the cytoplasm adjacent to the retained interphase nuclei. DNA that is packaged into micronuclei is then degraded as the embryo develops, presumably to avoid the previously discussed issues of misexpression. These mechanisms are initiated at the 7th cell division and are complete mostly by the 3rd day post fertilization, although micronuclei may be still be present. On the second day of embryonic development, the embryo undergoes the transition from blastula stage to gastrula stage, therefore, cells are initiating gene expression events that establish the earliest cell identities within the embryo and set the stage for the development of the primary germ layers. This increase in number and types of cells containing somatic DNA means that PGR must take place for these cell divisions to occur to allow for a

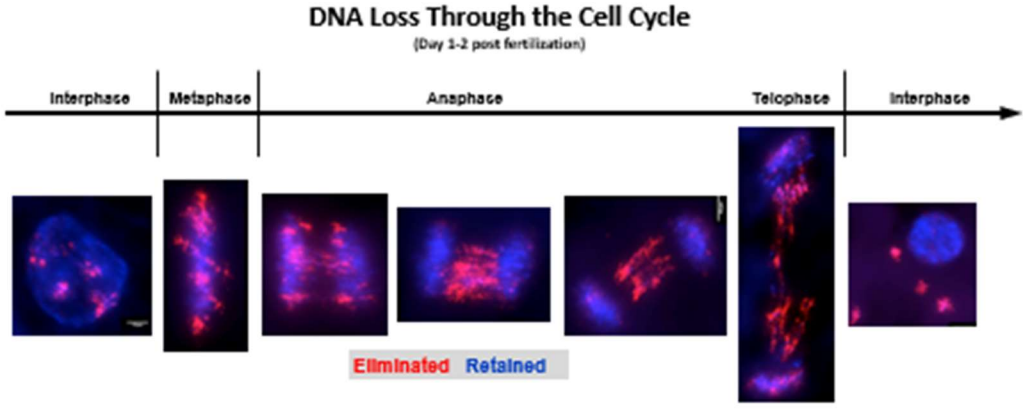

Figure 1. In PGR lagging chromatin is packaged into micronuclei and marked for deletion to restrict these genes from somatic expression [1].

germline-specific genome. Therefore, day two of development is when the most DNA is eliminated [1].

The cellular mechanisms of PGR are not yet fully understood; however, the knowledge of mammalian epigenetics can be applied to the lamprey genome to find genes of interest in PGR. In epigenetics, DNA methylation and histone methylation and acetylation are used to activate and inactivate transcription. At the most fundamental level, DNA can be defined as being packaged into heterochromatin (inactive) and euchromatin (active). Although previously understood to be "junk DNA" heterochromatin has been found to be involved in gene silencing, domain spreading, dispersion of effector regulatory proteins, and in relation to nucleolus organizer region (NOR) sequences, mitosis regulation and cell proliferation [4]. Therefore, the processes by which heterochromatin is regulated are necessary for cellular mechanisms as in PGR. This post-translation modification of DNA can occur through acetylation, methylation, phosphorylation, ubiquitination, and sumoylation, of which histone methylation is the most commonly addressed [5]. Histone methylation occurs through histone methyltransferases which add a methyl group to a specific site on the histone, eliciting differing effects dependent on the location of the methyl group. In addition to the location of the methyl group, the degree to which it is methylated i.e. mono-, di-, or trimethylated, also affects the level of gene silencing or transcription. Specifically, the H3K9 and H4K20 sites undergo methylation which results in gene silencing. The degree of methylation, particularly in H3K9, denotes the state of the corresponding gene. Monomethylation of H3K9 can denote early stages of X-chromosome inactivation, whereas trimethylation can denote pericentric heterochromatin, rarely ever transcribed due to its positioning near the centromere [5]. The involvement of genes within these mechanisms of silencing portray a possible interaction of corresponding genes in lamprey with PGR mechanisms.

In this study, two genes were investigated to determine the effects on PGR in lamprey. The suppressor of variegation 4-20 homolog 1 and 2 (SUV420H1/2), of which the protein is Histone-lysine N-methyltransferase KMT5B in humans was the first gene identified for analysis. The methyltransferase is involved in trimethylation of Histone 4 at Lysine 20 (H4K20). This methylation site is important in DNA damage response and is associated with heterochromatic regions, therefore it is a gene of interest when investigating programmed genome rearrangement [6]. In PGR, portions of the organism's genomic DNA are deleted which could be recognized as sites of DNA damage. In order to "repair" the DNA, the damage response must be initiated. When H4K20 is not correctly methylated, cells are not able to survive after DNA damage, specifically shown by the introduction of hydroxyurea, camptothecin (a topoisomerase I poison), ionizing radiation, and ultraviolet light [7]. In particular, SUV4-20H1/2 is involved in the DNA damage checkpoint. This G2-specific checkpoint is initiated by Crb2 and Rad proteins at the damage site. When the cell fails to pass this checkpoint, the transition from the second growth phase into mitosis is delayed to allow for the damage to be repaired through homologous recombination or excision repair [7]. Therefore, SUV420H1/2 has a significant role in facilitation of the DNA damage response which could then affect levels of PGR when SUV420H1/2 is suppressed.

The suppressor of variegation 3-9 homolog 1 (SUV39H1) which codes for the Histone-lysine-N-methyltransferase SUV39H1 was the second gene studied for its effects on PGR. Due to the association of PGR with methylation and gene silencing, SUV39H1 was identified as a gene of interest. The methyltransferase translated from SUV39H1 is responsible for catalyzing

di- and tri-methylation of histone 3 lysine 9 (H3K9)[8]. This particular position is a significant marker for heterochromatic DNA, demonstrating that this protein may have an important role in marking the germline DNA for deletion in the early mechanisms of PGR. H3K9 is also an important marker for chromatin packaging [8]. Previous studies have also demonstrated that when SUV39H1 is over-expressed, the number of micronuclei significantly increases along with defects in chromosome segregation [9]. This overexpression delays mitosis and consequently cell growth, portraying the involvement of SUV39H1 in cell division and possibly PGR. When embryonic lamprey cells divide, during anaphase, lagging chromatin can be observed. This chromatin is subsequently packaged into micronuclei and eventually degraded. The involvement of SUV39H1 in mitosis and chromatin packaging possibly connects this gene with PGR.

To assess the involvement of these genes, embryos with targeted mutations and their wildtype siblings will be imaged with light-sheet fluorescence microscopy with the Zeiss Lightsheet Z.1. The use of this machine allows for 3D images of the embryo, demonstrating the change distribution of micronuclei throughout each embryo. An issue for embryonic images is the lack of depth and focus within a reasonable time limit. Light-sheet fluorescence microscopy (LFSM) helps to overcome these shortcomings with the use of a wide-field microscope, lasers, a sheet of light, and a camera. The sample, an embryo embedded in agarose gel, is placed into view of the wide-field microscope, and a sheet of light illuminates the sample [10]. The sheet of light is critical to ameliorate the issues with focus; only the region in focus is illuminated, producing a signal for imaging. This process is continued through the sample with both a leftward and rightward facing laser providing two separate images. These two images can then be combined to produce a full 3D image of the embryo, depicting the spatial distribution of cells and consequently micronuclei.

Methods

Passive Clarity Technique (PACT)

Lamprey embryos have an extremely opaque yolk, posing as an obstacle in regard to imaging and subsequent analysis. The point of using CRISPR-mediated knockouts is to determine whether a specific gene influences the presence of micronuclei as a proxy for rate of PGR. As previously determined, the most efficient means for analysis involves imaging, but the embryos must be cleared for this to occur. As a solution, the PACT protocol as described in Yang et al. and further optimized for sea lamprey in Timoshevskiy et al. was used. MEMFA fixed Embryos that had previously undergone CRISPR-mediated knockouts for SUV420 H1/2 and SUV39H1 as well as sibling controls were cleared using this PACT technique. The embryos were gradually brought out of methanol with 1xPBS and then placed in hydrogel monomer solution (5% acrylamide supplemented with 0.5% VA-044) at 4℃ overnight on a nutator. To allow for hydrogel polymerization, the embryos were then incubated at 37℃ with gentle rotation for 3 hours. After incubation, the embryos were briefly washed with 1xPBS and then changed into stripping solution (8%SDS in 1xPBS) and incubated at 37℃ with gentle rotation for 5 days. At the conclusion of this incubation period, the embryos had been successfully cleared. To prepare for staining, the embryos were washed with 1xPBS 5 times, changing solution each time and then transferred into staining solution (1xPBS, pH=7.4, 0.1 Triton X-100, 0.01% sodium azide). SYTO 21 dye was also added and the embryos were left protected from light at room temperature overnight. The stain did not sufficiently take with the first addition, therefore dye

was administered and left overnight protected from light at room temperature for a second time. The DNA was sufficiently stained after the second addition of dye. At the conclusion of clearing and dying the embryos were left at room temperature before microscopy and DNA extraction.

Light-sheet Microscopy

Light-sheet microscopy was completed for five embryos in each category: SUV39H1 controls, SUV39H1 knockouts, SUV420H1/2 controls, and SUV420H1/2 knockouts. After immersing embryos in RIMS solution, 5 embryos were embedded in 2.5% agarose gel, pulled through a capillary tube and set at 4℃ for no less than 5 minutes. After successful embedding, the embryos were placed into the LSFM machine, and pushed out one at a time into the RIMS solution for imaging. The image was taken with the 5x objective lens with dual-sided laser illumination. Having a laser capturing either side of the embryo minimizes the risk of missing any cellular information. Following imaging, the resulting image was split in half with the respective laser as the only source of illumination. These halved images included an extra 90 pixels on either side to account for alignment. These images were then stitched back together after aligning in the x, y, and z planes. To obtain numerical results, pipelines to count nuclei, micronuclei, and notate the associations between nuclei and micronuclei were run for each embryo through the Arivis software.

Microscopy Imaging

For analysis of embryos, images obtained were analyzed through CellSens software. Manual counts were completed of each embryo, ranging from 400-550 cells per embryo. These counts were completed by adjusting the image to 100 micrometer scale and beginning at the top right of the image and snaking up and down the image to ensure accurate counting. Once the counts were half completed, counting shifted to the bottom left of the image and snaking inwards until 400-550 cells were counted. Data input was completed in a binary system for presence of micronuclei, along with a respective number of micronuclei present. To proceed with data analysis, nuclei were sorted based on micronuclei presence and converted into proportions.

DNA Extraction and PCR

To confirm that the knockouts had been successful, the DNA was extracted from all imaged embryos through the use of the MagJET Genomic DNA Kit and used for PCR. PCR was run with a 60℃ annealing temperature for 34 cycles with a final 30 second extension period after completion of cycling.

Results

SUV420H1/2

The first facet to this study included the effect of SUV420 CRISPR-mediated knockouts on the number of micronuclei present in lamprey embryos. This was studied through images created through microscopy and then uploaded to CellSens

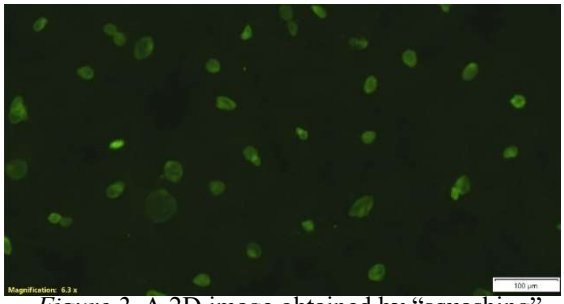

Figure 2. A 2D image obtained by "squashing" an embryo on a slide. The nuclei and micronuclei seen were counted for comparative analysis.

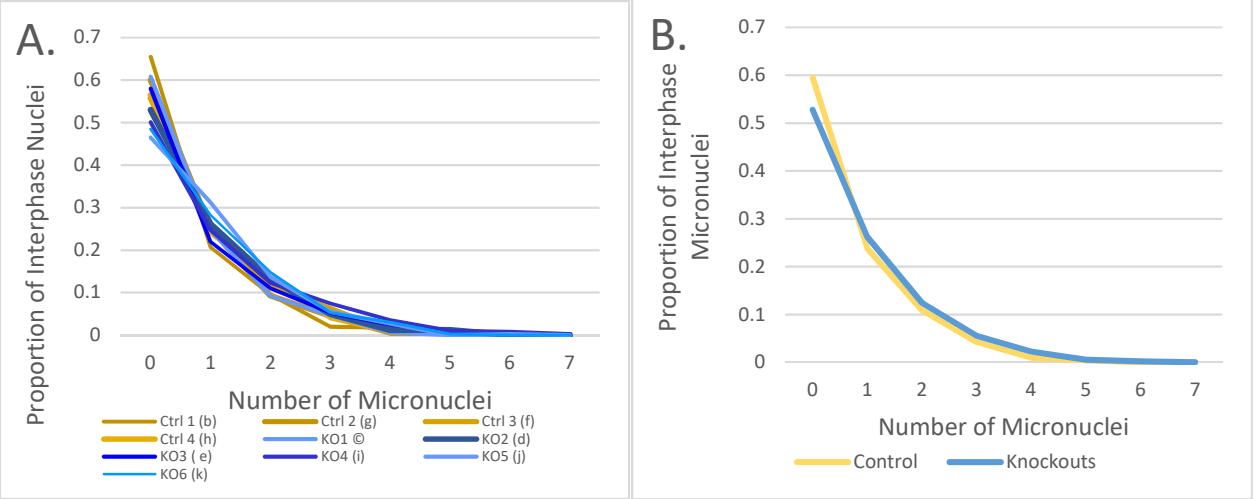

Figure 3. A. The raw data results per embryo are demonstrated with the knockout embryos in blue and controls in yellow. B. The averages of both control and knockout embryos are shown, depicting the general similarity in data.

Imaging Software as shown in Figure 2. The results, depicted in Figure 3, do not show a significant difference in the number of micronuclei present per nucleus when comparing the control and knockout embryos. This data only includes interphase cells because that is when micronuclei are easiest to confidently identify. During data collection, few cells were seen in anaphase demonstrating lagging chromatin. This observation further verifies the formation of micronuclei from lagging chromatin. The data collection for knockout embryos that occurred later in analysis had increased proportions of micronuclei per interphase nucleus when compared to earlier control and knockout embryos. Had a positive or negative significant difference been observed, the gene would have been associated with an effect on the mechanisms of PGR. For SUV420H1/2 the effect would have largely been in the damage response checkpoints to allow for cellular division following DNA deletion. Since the direct difference was not observed, an immediate association did not occur; however, due to the intriguing trend of increase of micronuclei as data collection time increased, human error may have been involved. With the possible observation of human error, further steps were taken to determine whether SUV420H1/2 influences micronuclei formation.

New control and knockout embryos were cleared and imaged with light-sheet microscopy to obtain a definitive answer. Light-sheet microscopy provides a wholistic view of the embryo compared to the 2D image resulting from “squashing” the embryo onto a microscope slide. This 3D view provided an interesting look into the dispersal of cells and nuclei within a day 2 lamprey embryo as seen in Figure 4.

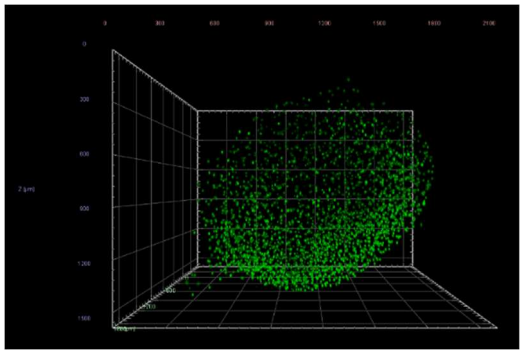

Figure 4. A 3D view of a stitched light-sheet image of an SUV39H1 knockout embryo. This image demonstrates the dispersion of nuclei and micronuclei across a D2 embryo.

Following the completion of analysis of the light-sheet images, it can be confidently stated that SUV420H1/2 does have an effect on programmed

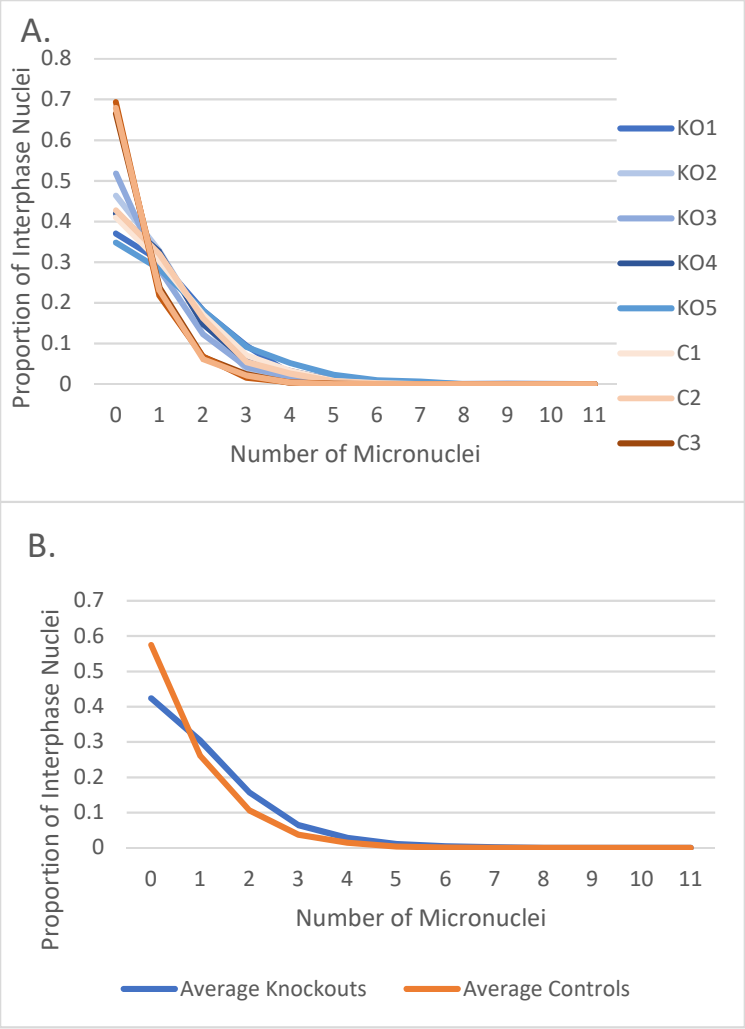

Figure 5. **A.** The proportion of interphase nuclei as a function of the number of micronuclei for each embryo analyzed. **B.** The mean proportion of interphase nuclei as a function of micronuclei for SVU420H1/2 knockouts and sibling controls. Knockouts in blue and controls in orange.

genome rearrangement. As shown in Figure 5, the control embryos had approximately between 40% and 70% of interphase nuclei with 0 micronuclei, compared to the range of 34% to 52% for the knockout embryos. The range would be much smaller the control embryos; however, Controls 1 and 2 were ripped in the process of embedding in the agarose gel for light-sheet microscopy. Once ripped, some parts of the embryo were likely not sensed when imaging took place, resulting in less precise results pertaining to the proportions of nuclei with and without the presence of micronuclei. Despite this inconsistency, the entire sample size is large enough to account for this variation and provide accurate results. As the number of micronuclei increases, the proportion of interphase nuclei decreases as expected; however, the SUV420H1/2 knockouts have an increased number of nuclei with micronuclei indicative of differing levels of PGR. There were 12166 knockout nuclei counted, and 13384 control nuclei counted, providing means for a significant p-value. The total observed 7109 nuclei with micronuclei (proportion=0.584) was compared with the expected 4784 nuclei with micronuclei (proportion=0.393) for a x^2 value of 1129.884 (degrees of freedom=1). This value corresponds to a p-value of 5.2869×10^{-248}. Therefore, there is a significant difference between the knockout number of nuclei with micronuclei and the expected number from the control embryos. This p-value is extremely small due to the large sample size and use of 1 degree of freedom due to the use of the total nuclei observed. Conclusions drawn from the 2D and 3D imaging are seemingly different; however, following further analysis, the same trend is seen in both datasets. The difference between knockout and controls embryos is more considerable due to the increased sample size (from 500 cells to the entire embryo which is approximately 3000 cells). The significant p-value paired with a similar trend seen in multiple sets of knockout embryos signifies that SUV420H1/2 has a role in PGR mechanisms. The number of micronuclei was a proxy for the level of programmed genome rearrangement occurring. When SUV420H1/2 is not present, micronuclei numbers are

higher than expected demonstrating that the effect could be mechanistic or developmental. Regarding the mechanistic aspects of PGR, SUV420 could be involved in the regulation of micronuclei production. Typically, more cells have smaller amounts of larger micronuclei, allowing degradation to be localized and less energy input into the production of many micronuclei. The trend of cells having an increased number of more micronuclei indicates that SUV420H1/2 could be a part of the production of the micronuclei themselves, or a regulatory factor that controls the number of micronuclei produced as the cells progresses from anaphase to the subsequent interphase. When taking into account the role of SUV420H1/2 in the cell, DNA damage G2 checkpoint, it can be inferred that this role would more likely be within the developmental aspects of PGR. Without the activation of SUV420H1/2, the G2 checkpoint has a decreased capacity for cell cycle regulation. Cells with incorrectly repaired DNA maybe be allowed to proceed through mitosis, therefore replicating the mutated genome. This could result in larger amounts of DNA marked as lagging chromatin, allowing for its eventual exclusion from the nucleosomal envelope in cytokinesis. Increased amounts of lagging chromatin will result in a greater number of micronuclei throughout the embryo. This will be further tested through the application of genetic probes for expected genome deletion. The resulting micronuclei in the SUV420H1/2 knockouts can then be analyzed for the presence of DNA not containing the probes, and therefore should not be contained in the micronuclei. If unmarked DNA is present, then it can be concluded that SUV420H1/2 is a part of the PGR mechanism in regard to the confirmation of the germline-specific sequences as a part of lagging chromatin. If this is not observed, then the mechanistic aspect of micronuclei production regulation can be investigated through examination of micronuclei size to demonstrate its role in regulating the number of micronuclei produced.

SUV39H1

The control and knockout SUV39H1 embryos were only analyzed through light-sheet microscopy, providing comprehensive analysis. A total of 15893 knockout nuclei and 15733 control nuclei were counted, massive and similar sample sizes for each treatment. Overall, Figure 6 depicts a trend different than that of SUV420H1/2. The control embryos had more nuclei with micronuclei as well as more nuclei with larger numbers of micronuclei. The total mean proportion of interphase nuclei with micronuclei is 0.656 (10467/15893) for the knockout embryos and 0.79 (12430/15733) for the control embryos. These values and their respective proportion of nuclei without micronuclei were used to test the statistical significance of this data in reference to the hypothesis that the knockout of SUV39H1 has an effect on the proportion of nuclei with micronuclei. The observed number of nuclei with micronuclei was 10467, the expected (through the use of the total mean proportion) was 12556.41. This resulted in a x^2 value of 347.6815 (degrees of freedom=1) and a p-value of 6.796×10^{-78}. Therefore, it can be concluded that there is a statistically significant decrease in micronuclei in the knockout embryos compared to the control embryos. This p-value is exceptionally low due to the sample size of 15893 knockout embryos and the use of 1 degree of freedom as a result of the use of the total mean. A significant difference relates to SUV39H1 being an important component in PGR. When SUV39H1 is not present, the cells generally had smaller numbers of micronuclei, if any were present. This denotes that the effect of SUV39H1 on PGR lies either in the production of micronuclei, or in the segregation of lagging chromatin. With the smaller proportion of nuclei with micronuclei, SUV39H1 could be involved in the packaging of the lagging chromatin into micronuclei. With knockout of SUV39H1, the embryo was possibly not as successful in the

production of micronuclei, resulting in the lower proportion. The association of SUV39H1 as a marker for chromatin packaging would explain this relationship. Packaging chromatin into micronuclei could occur due to a similar mechanism of packaging chromatin into chromosomes, so without SUV39H1 allowing for a marker for packaging, less micronuclei were able to be produced.

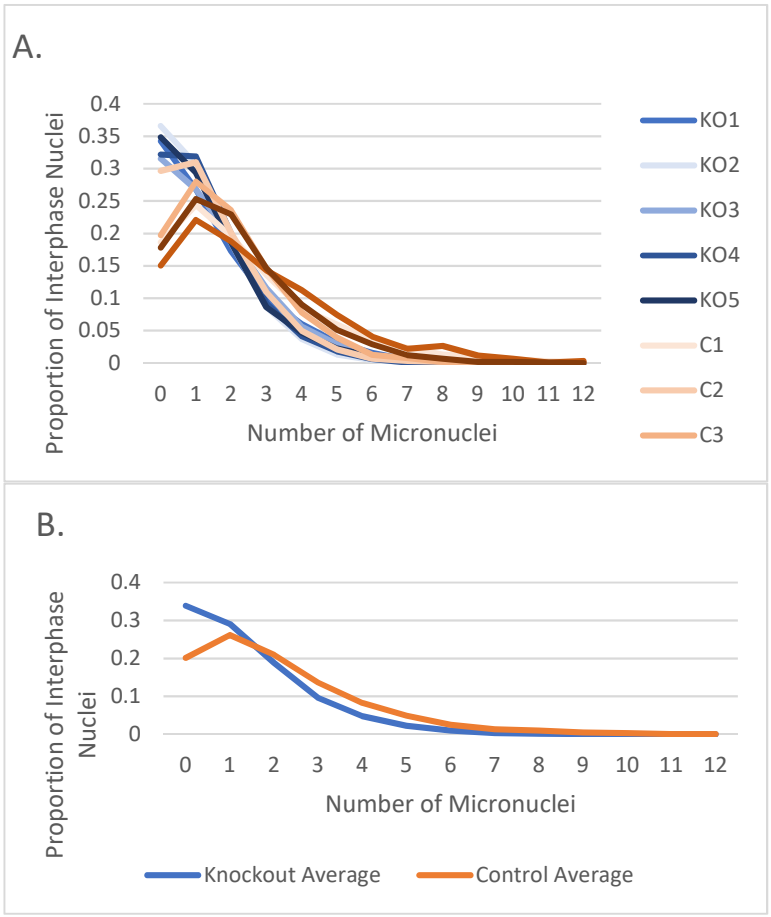

Figure 6. **A.** The data from all 10 analyzed embryos are represented in this chart with knockouts in blue and controls in orange. **B.** The mean proportions of interphase nuclei with the respective number of micronuclei are portrayed. Through the use of averages, significant differences can more clearly be seen.

The second explanation, an effect on the segregation of lagging chromatin into micronuclei is also plausible due to the role SUV39H1 in chromosome segregation. As a cell progresses from metaphase into anaphase, the DNA is pulled to opposite ends of the cell, ultimately separating the replicated DNA into what will be two distinct cells. The chromosomes are segregated to allow for this separation; however, the chromatin that is not "pulled" to the end becomes the lagging chromatin. Chromosome segregation to allow for lagging chromatin would be significantly affected by the knockout of SUV39H1. With a decreased ability of a cell to segregate genetic material to eventually be included in micronuclei, an observation of decreased number of micronuclei would be expected. Due to this observation in the results of this study, the role of SUV39H1 may be within the area of genetic material segregation. To confirm this mechanistic role, genetic probes for the germline specific DNA should be used to determine if all germline specific DNA is being separated out into the micronuclei. If a significant number of nuclei still contain germline specific DNA in SUV39H1 knockouts compared to the sibling controls, then it can be concluded, after PCR confirmation of knockout success, that SUV39H1 is involved in programmed genome rearrangement in the capacity of lagging chromatin segregation.

An interesting facet was also uncovered through the production of this figure. The controls had a smaller proportion of interphase nuclei with no micronuclei compared to proportion of interphase nuclei with 1 micronucleus. This has not been observed before in day 2 embryos, directing towards an assumption that these embryos were possibly harvested at an

earlier stage of embryogenesis. The peak of PGR activity is during day 2 when the transition from blastula to gastrula takes place; however, the controls seem to have a greater amount of PGR activity in respect to the proportion of nuclei with micronuclei being an average of 0.79. As the embryo moves from day 2 to day 3.5 of development when PGR is essentially complete, the total number of micronuclei first increases and then decreases as they are degraded. Therefore, these embryos were most likely harvested at a slightly earlier stage than the denoted day 2 harvest; however, the effect on the overall results is negligible due to the magnitude of the statistical significance.

The underlying assumption that presumptive knockout embryos carried mutations within their target genes was tested by PCR and gel electrophoresis. Forward and reverse primers were designed for the CRISPR targeted SUV39H1 sequences and verified on control sperm and blood DNA. The extracted DNA of all 10 embryos was used in the PCR and visualized through gel electrophoresis. Through multiple runs of the DNA, it was determined that the knockout of SUV39H1 was successful (Figure 7 A). As seen in lanes 8-12, bands shorter than the primer sequence of 578 bp and multiple bands denote that the SUV39H1 sequence is not present. In lanes 2-6, the majority of control embryos have bands with a size of 578 bp, demonstrating that the SUV39H1 sequence is present. In Figure 7 B, the gel electrophoresis for SUV420 controls and knockouts were also demonstrative of the presence of the CRISPR-targeted sequences in controls and the introduction of mutations in knockout embryos. Since it was confirmed that the control embryos contain the sequence and the knockouts carry versions with altered sizes for both genes, the differences between the control and knockout embryos can be attributed to the lack of SUV39H1 and the lack of SUV420 respectively.

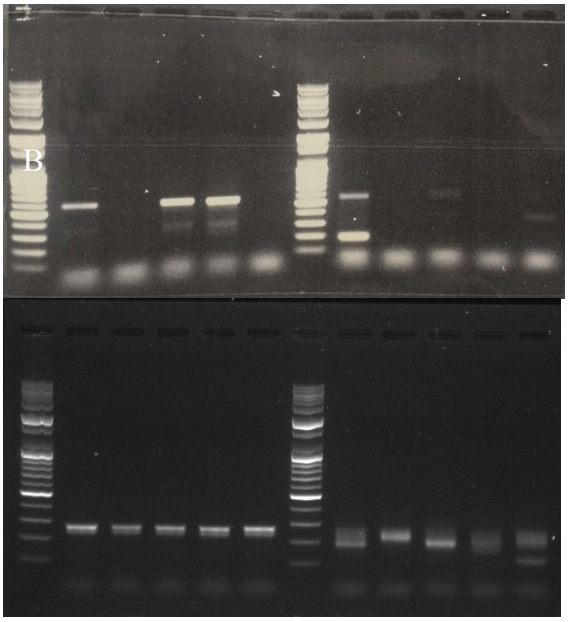

Figure 7. A. Gel Electrophoresis of SUV39H1 control and knockout embryo PCR. Lanes 2-6 contain DNA from the 5 controls and lanes 8-12 contain DNA from the 5 knockouts. Variation in band sizes is consistent with the presence of g B. Gel Electrophoresis of SUV420 control and knockout embryo PCR with the same setup as above.

Conclusion

Through this study, it has been determined that both SUV420H1/2 and SUV39H1 genes are likely involved in PGR in some capacity. To further these findings, experiments to confirm the reason for the effect will be performed including the use of genetic probes for the germline specific DNA sequences. In addition to the SUV39H1 and SUV420H1/2 genes, I will study knockouts of genes with similar associations with heterochromatic markers. Both genes studied served as major heterochromatic markers, H4K20 and H3K9. Due to the significant results, continuing this study by using knockouts of genes associated with gene silencing and methylation would be a suitable next step. The results of the SUV39H1 controls pose an interesting look into the progression of micronuclei formation as the embryo develops. A second facet for next steps would be to delve into precise expected proportions of nuclei with micronuclei as an embryo develops. Currently, we have a general idea, that embryos have peak amounts of PGR

throughout day 2, and then the micronuclei are degraded as the embryo develops past day 3. Having a baseline proportion distribution would be helpful to have a greater understanding of the PGR timeline and a second control aspect to compare future knockout embryos.

Recent studies in the lab have also suggested that programmed genome rearrangement occurs in other vertebrate taxa, such as elephant shark. The elephant shark genome is much easier to work with due to its significantly smaller number of repeats when compared to the sea lamprey genome. The respective genes of SUV420H1/2 and SUV39H1 could also be investigated in elephant shark to determine if their effect on PGR occurs in multiple species or just sea lamprey. Through the comparison of PGR in sea lamprey and elephant shark, a universal mechanism for PGR can be further developed. Once PGR is better understood, the beneficial aspects would eventually be applied to humans. Lamprey have germline specific genes mainly to protect themselves from oncogenesis. The deleted genes are involved in pluripotency, therefore, if mutated, have strong deleterious effects. Once understood, PGR mechanisms could then potentially be used for therapeutic treatments, specifically concerning cancer.

References

1. Timoshevskiy, V.A., et al., *Cellular and Molecular Features of Developmentally Programmed Genome Rearrangement in a Vertebrate (Sea Lamprey: Petromyzon marinus).* PLoS Genet, 2016. **12**(6): p. e1006103.
2. Smith, J.J., et al., *The sea lamprey germline genome provides insights into programmed genome rearrangement and vertebrate evolution.* Nat Genet, 2018. **50**(2): p. 270-277.
3. Smith, J.J., et al., *Genetic consequences of programmed genome rearrangement.* Curr Biol, 2012. **22**(16): p. 1524-9.
4. Boisvert, F.M., et al., *The multifunctional nucleolus.* Nat Rev Mol Cell Biol, 2007. **8**(7): p. 574-85.
5. Krishnan, S., S. Horowitz, and R.C. Trievel, *Structure and function of histone H3 lysine 9 methyltransferases and demethylases.* Chembiochem, 2011. **12**(2): p. 254-63.
6. Yang, H., et al., *Preferential dimethylation of histone H4 lysine 20 by Suv4-20.* J Biol Chem, 2008. **283**(18): p. 12085-92.
7. Sanders, S.L., et al., *Methylation of histone H4 lysine 20 controls recruitment of Crb2 to sites of DNA damage.* Cell, 2004. **119**(5): p. 603-14.
8. Wang, T., et al., *Crystal structure of the human SUV39H1 chromodomain and its recognition of histone H3K9me2/3.* PLoS One, 2012. **7**(12): p. e52977.
9. Melcher, M., et al., *Structure-function analysis of SUV39H1 reveals a dominant role in heterochromatin organization, chromosome segregation, and mitotic progression.* Mol Cell Biol, 2000. **20**(10): p. 3728-41.
10. Power, R.M. and J. Huisken, *A guide to light-sheet fluorescence microscopy for multiscale imaging.* Nat Methods, 2017. **14**(4): p. 360-373.